SEMARAK ILMU PUBLISHING

Journal of Advanced Research in Fluid Mechanics and Thermal Sciences

Journal homepage:
https://semarakilmu.com.my/journals/index.php/fluid_mechanics_thermal_sciences/index
ISSN: 2289-7879

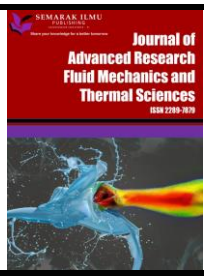

Numerical Investigation of using FDCU on Temperature Distribution in Non-Unidirectional Cleanrooms

Ayman Abd Elsattar Elsaey[1,*], Mahmoud Ahmed Fouad[1]

[1] Mechanical Power Department, Faculty of Engineering, Cairo University, Giza, Egypt

ARTICLE INFO

Article history:
Received 28 November 2022
Received in revised form 13 March 2023
Accepted 20 March 2023
Available online 7 April 2023

Keywords:
FDCU; FFU; Fan Dry Coil Unit; innovative ventilation system

ABSTRACT

Cleanrooms are used in a lot of industrial applications, one of which is the field of electronic industries. Manufacturing process tools that equip the cleanroom and are used in this field dissipate a lot of heat in all room areas. This work presents a 3D numerical simulation for a recently published experimental work that proposes an innovative fan dry coil unit (FDCU) return air system. This system consists of ceiling supply fan filter units and ceiling return fan coils. Throughout the research, a comparison of temperature distribution between the FDCU return air system and the traditional wall return air system is presented. Moreover, the effect of changing the FDCU location on the cleanroom ceiling is investigated. To validate the numerical simulation results, a direct comparison is performed with the experiment data, and the numerical model shows good agreement. The results show that FDCU ARR-3 is the best arrangement compared to other models, namely wall-return, ARR-1, and ARR-2. The AVG local air temperature index Θ through the cleanroom was reduced by 77% compared to wall return and 33% compared to ARR-1. Moreover, the AVG local air temperature index Θ above the process tool was reduced by 28% compared to a wall return and 23% compared to ARR-1.

1. Introduction

The advancement of several production technologies over the past few years' aids in the scaling down of devices into the nanoscale generation, increasing the sensitivity to the contamination of particles into sub-micron regions. According to that cleanroom obtained a big concern due to its importance in the electronic manufacturing industry [1-3]. The majority of cleanrooms are occupied with process tools that emits high-temperature heat and particles, increasing airflow resistance above normal levels and lower the quality of the cleanrooms. This increases the number of studies on cleanrooms used for numerous industries [4,5]. Traditional cleanroom airflow pathways rely on installing fan filter units (FFUs) to introduce supply air from ceilings and extract return air through return air shafts (RASs) and wall-return air grilles. Tung *et al.,* [6] studied the airflow characteristics and its effect on particle removal in a cleanroom equipped with tools arranged in different floor

* *Corresponding author.*
E-mail address: aymanelsaey@gmail.com

https://doi.org/10.37934/arfmts.105.1.1530

covering configurations and using different air return system opening arrangements. Even though the return air plenum drives up the cost of construction, the wall-return air system has various shortcomings. The need for high external static pressure for FFUs airflow to get through the wall-return passage resistance. Moreover, fixed placements of the wall-return air grilles openings add to the uneven temperature distribution due to the interaction between the hot air current from tools and the cold air current from the ceilings [7]. With the increasing application of fan filter units (FFUs) in semiconductor manufacturing a lot of research has focused on improving the performance of FFUs because of their flexible installation [8-10]. Zhao *et al.,* [11] proposed a new control strategy of fan filter units (FFUs) based on personnel location within the cleanroom to reduce the operating air volume. Shao *et al.,* [12] performed a study in an unoccupied cleanroom to demonstrate the effects of partial FFUs in preventing local particle pollution.

Several numerical and experimental studies on the traditional wall-return system showed that contaminant particle sizes smaller than 4.5 μm in diameter having no gravitational sedimentation effect on the diffusion [13-15]. Kato *et al.,* [16]. Presented a technique for balancing the supply and exhaust airflow rates at the ceiling. This ventilation system is designed to prevent the establishment of recirculating flow over the entire space, and more effective contamination exhaust in cleanrooms. Lin *et al.,* [4,7] have proposed an innovative fan dry coil unit (FDCU) return air system, consisting of ceiling-supply and ceiling-return fan coils. Investigation of air changes per hour (ACH) and SAP pressures on the removal of 0.1 μm particles was performed. The study reported that the FDCU-return air system can exhaust more than 50% of particles from the cleanrooms, compared with the conventional wall-return air system. Furthermore, it is advised that the configuration of the FDCU-return ventilation system be taken into consideration to increase the efficiency of eliminating particles from the industrial cleanrooms. Air change rate (ACH) plays a significant role in the indoor airflow field, with a notable impact on the deflection and distribution of thermal plume [17]. Qin and Lu [18] proposed positioning the exhaust near the thermal plume to efficiently remove heat from a large office cooled by an IJV system.

The effect of turbulence has been noted by Ljungqvist [19] who pointed out that even at a low speed, 0.2 m/s, turbulence is still created in the room and plays an important role in the diffusion process of the gases and particles. Milberg *et al.,* [20] noticed that as the air turbulence increased from 1 to 10%, the number of larger particles (>0.33 pm) deposited on the surfaces was increased by 39% and 46%. Zhao *et al.,* [21] derived a theoretical expression for the clean air volume in a non-uniform cleanroom environment by treating particle transport as passive transport and utilising the accessibility index to define the effect of particle sources on the clean zone.

Kuehn [22] and Kuehn *et al.,* [23] measured the air velocities and turbulence behaviour in a full-scale vertical laminar flow (VLF) type clean room by using a 1-D hot wire anemometer. Fujii *et al.,* [24] reported the air flow turbulence behaviour inside a clean booth without any equipped devices and based on the 2-D turbulence data. Hu *et al.,* [25] employed a three-dimensional ultrasonic anemometer to evaluate the non-homogenous nature of the airflow under the ULPA filter and turbulence generated by different equipment and facilities of the FFU-type cleanroom. Lin *et al.,* [5] proposed an Innovative fan dry coil unit (FDCU) return air system and investigated the impact of manufacturing process tool heat dissipation on temperature distribution and airflow characteristics in cleanrooms. The study shows that this system is superior to a traditional wall-return air system in successfully removing sub-micron particles and can greatly improve air motion characteristics and temperature distribution. Whyte *et al.,* [26] investigated airflow characteristics in a non-unidirectional airflow cleanroom and studied its effect on cleanliness level. Concluded that a turbulent intensity of 6% and a hydraulic diameter derived from the full size of the air inlet gave the closest results to the actual airflow field. Lin *et al.,* [27] investigated by experiment a cleanroom

equipped with an FDCU-return system to another equipped with a conventional wall-return system to evaluate the energy efficiency. Results indicated that the FDCU-return system can improve energy efficiency and reduce power usage by more than 4%.

This research concerns the effectiveness of using FDCU as suggested return air system compared with traditional wall return. Most of the previous studies focused on the effect of using such system on temperature distribution, air flow characteristics, contaminant exhaust and energy saving. Studying the effect of FDCU openings arrangement on temperature distribution has not been performed elsewhere.

2. Model Verification and Validation

2.1 Experiment Description

The model is validated through comparison to the experimental work of Lin *et al*., [5]. The experiment depicted in Figure 1 is a full-scale cleanroom measuring 4.8 m (L), 6.3 m (W), and 2.8 m (H) in the X, Y, and Z directions, and configured at 23.5 °C and 45% relative humidity (RH).

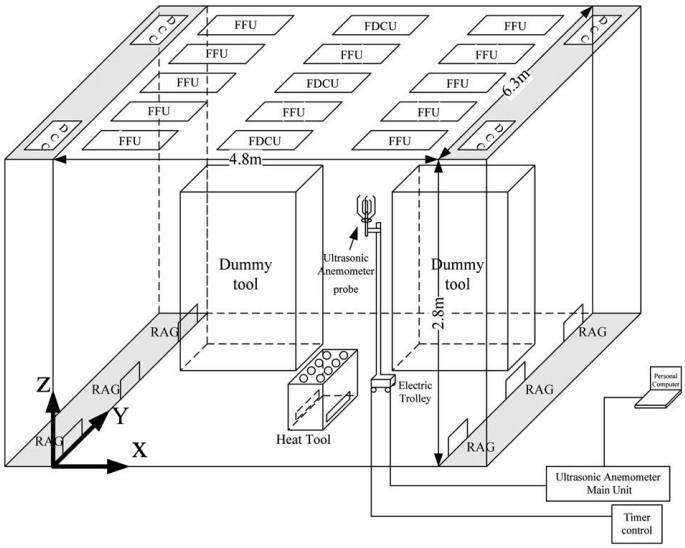

Fig. 1. Configurations of a full-scale cleanroom

The cleanroom contained two dummy tools with dimensions of 1.6 m (L), 1.2 m (W), and 2.4 m (H), as well as a manufacturing tool measuring 0.9 m (L), 0.6 m (W), and 1 m (H).

To investigate the collision between the rising hot exhaust from the manufacturing process tool and the downward cold air from the FFUs, the manufacturing tool was precisely positioned under one of the FFUs, with its centre located at X = 2.4 m and Y = 1.8 m in the X and Y directions, respectively. Twelve FFUs with dimensions of 1.2m L, 0.6m W and 0.275m W comprised the supply air grilles as shown in Figure 2. In addition to the FFUs, ULPA filters were installed. In Figure 3, an FDCU measuring 1.17m L, 0.57m W, and 0.45m H is illustrated schematically. On the ceiling, three parallel arrays of FDCUs and FFUs were installed. For the sidewall return, three pairs of RAGs and two pairs of DCCs were installed.

Upon activation of the process tool, the supply air velocity of FFUs corresponded to supply airflow rates of 120 and 130 ACH in the wall-return and FDCU-return air systems, respectively. The temperature and velocity of the tool's supply air were measured to be 45°C and 1.2 m/s, respectively. This study employed a local air temperature index $\Theta = (T_{local} - T_{in}) / (T_{return} - T_{in})$ to characterize how hot air exhaust from the manufacturing tool affected the temperature of indoor air at all locations

where the air temperature was measured. where Tin, T_{return}, and T_{local} refer to the temperature of supply air to the room, return air, and room air at any locations (℃), respectively. when Θ > 1 denotes the diffusion of hot air in the cleanroom, whereas Θ < 1 denotes the extraction of the majority of hot air from the cleanroom. More details can be found in Lin *et al.,* [5].

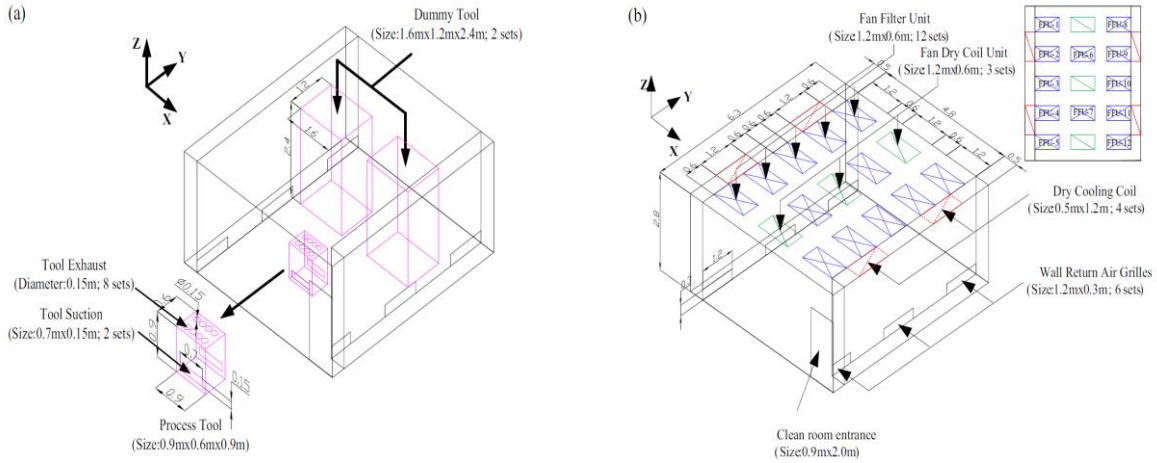

Fig. 2. Configurations of tools, wall-return, and the FDCU-return air openings

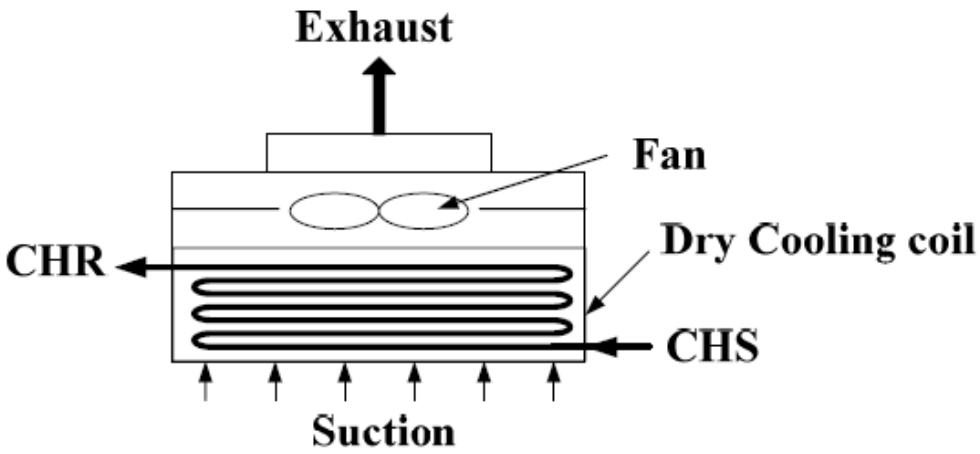

Fig. 3. Schematic diagram of an FDCU

2.1.1 Wall return case

All of the FDCUs depicted in Figure 1 were sealed with blind plates and switched off. The room air was delivered to the cleanroom from the SAP through the FFUs at a velocity of 0.36 m/s and a temperature of 23.1°C, exhausted from RAGs at a temperature of 25.6°C, and then introduced back to the SAP through RASs and DCCs. Throughout this cycle, DCCs were utilized to cool the returned air.

2.1.2 FDCU return case

All of the RAGs depicted in Figure 1 were entirely sealed with blind plates. The supply air was delivered from the SAP via the FFUs at a velocity of 0.38 m/s and a temperature of 22.6°C, while the return air was delivered via the FDCUs at a temperature of 24.6°C. During this air cycle, coils included

within the FDCUs were used to cool the returning air rather than the DCCs used in conventional wall returns.

2.2 Numerical Model Description

2.2.1 Solution domain description

The current domain Figure 4 and Figure 5 have the same dimensions as the experimental work. Lin *et al.,* [5]. A comprehensive examination of the numerical simulation results produced for typical wall return and FDCU ventilation systems employing the three different ARR-1, ARR-2, and ARR-3 exhaust configurations. The local air temperature index at various room cross-sections has been researched and plotted. Validating the numerical model with a conventional wall return ventilation.

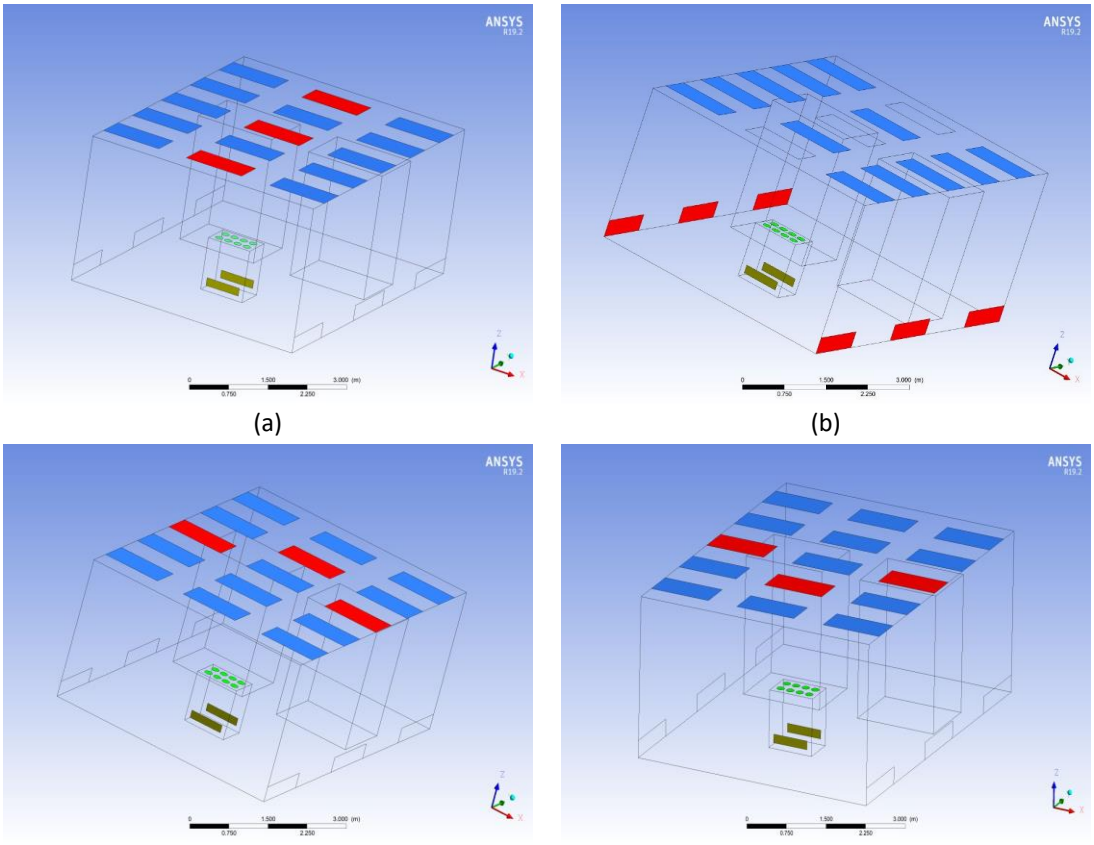

Fig. 4. Numerical models (a) Wall-return (b) ARR-1 (c) ARR-2 (d) ARR-3

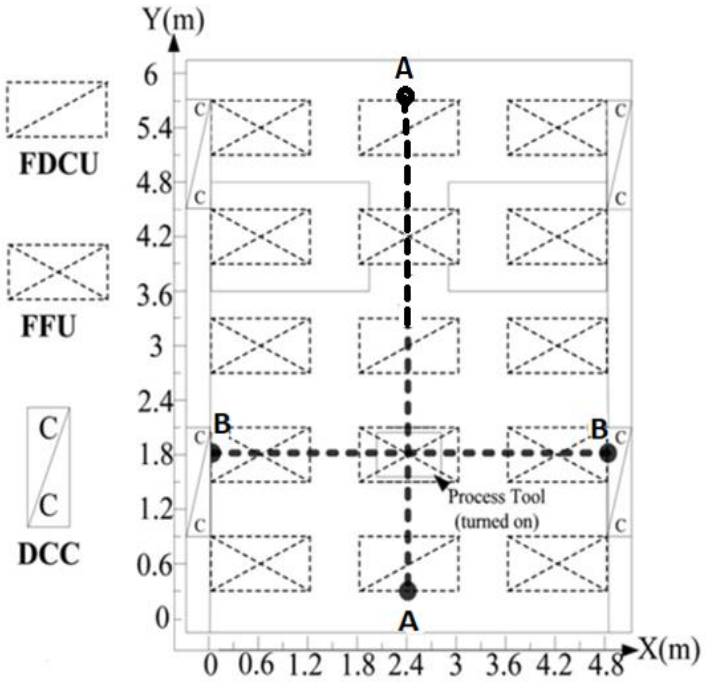

Fig. 5. Top views of the cleanroom with sections A and B

2.2.2 Numerical model and solution method

FLUENT, a commercial CFD software tool which was used in a variety of different cases [28-31], serves as the foundation for a numerical model (version 19.2 R). This general-purpose code is a Navier–Stokes solver for finite volumes. A 3D and steady-state CFD modelling methodology was created to explore the airflow characteristics and temperature distribution patterns within the room. The energy equations and realizable k- ε turbulence model with a standard wall function have been solved, and a SIMPLE algorithm for pressure-velocity coupling with standard pressure interpolation and first-order discretization for convective and viscous factors has been implemented.

2.2.3 Turbulence model

Fluent offers a vast selection of models for modelling air turbulence. With the available computing resources, the conventional k-ε model and its two versions, the realizable k- ε model and the RNG k- ε model, were the most applicable ones. The k- ω turbulence model was also available, but it did not appear to be a suitable option due to the boundary layer considerations that must be taken into account when using this model. Numerous trials have been conducted to evaluate the agreement between the numerical solution and experimental work. During these trials, the RNG k-ε turbulence model, the realizable k- ε turbulence model, and the k- ω two equations model have all been used, and the results indicate that the realizable k- ε two-equation model is the most suitable model for accurately simulating temperature distribution and airflow characteristics.

2.2.4 Boundary condition

The selection of boundary conditions is a crucial issue, especially in the present case study due to jet impingement caused by FFU and process tool exhaust jets coming from process tool operation. As determined experimentally [5], the process tool was reoriented to be projected beneath one of

the FFUs in order to analyse the most significant case of airflow characteristics and its effect on temperature distribution. The area above the process tool is a highly turbulent area resulting from the impact of hot, high-velocity air exhaust from the manufacturing process tool and the supply of downward cooled air from FFU. That is directly above the process tool.

Several experiments were conducted to determine the optimal set of boundary conditions that can accurately predict the flow characteristics while taking into account the large turbulence behaviour of the current case under investigation. The scientific literature on this subject is limited, and the best choice of turbulent intensity and hydraulic diameter to describe the boundary condition at the air supply inlet of a non-unidirectional airflow cleanroom is unclear, as if it is the best choice of turbulence model. These issues were investigated by comparing the experimentally produced airflow fields with those from CFD models by conducting numerous experiments with varied turbulence intensities of 1% and 6% and a hydraulic diameter of 0.8 m for the air inlet unit [26].

However, it was determined that a turbulent intensity greater than that observed in practice should not be employed in the CFD study, hence, a turbulent intensity of 6% was used throughout the CFD analysis. Table 1 summarizes the boundary conditions that are set up in the current study.

Table 1
The boundary conditions employed in the present study

Computational domain	4.8 m (x) × 6.3 m (y) × 2.8 m (z)
Air supply ports (FFU)	Vin= 0.36 m/s, Tin= 296.1℃ wall return case
	Vin= 0.38 m/s, Tin= 295.6℃ FDCU return case
process tool inlet	Vin= 1.2 m/s, Tin= 318℃
Clean room exhaust	Six exhausts; outflow with 0.95 %
Process tool exhaust	Two exhaust; outflow with 0.05 %
Top wall	Isothermal wall with no-slip condition
Side walls	Isothermal wall with no-slip condition
Dummy tools	Isothermal wall with no-slip condition
Process tool surface	Isothermal wall with no-slip condition
Process tool side wall	Isothermal wall with no-slip condition

2.2.5 Meshing technique of the numerical model

The computational domain is discretized using an ICEM CFD Ver. 19.2 hexahedron-structured mesh. Initially, the turbulence models were run in steady-state, which is the standard technique for many CFD problems. It was discovered, however, that the bulk of simulations failed to induce convergence of the solution far below 1×10^{-4} [26].

Poor meshing is a typical issue that inhibits good convergence. Due to the intricacy of the geometry, particularly in the exhaust process tool region, a tetrahedron mesh was initially employed in the current investigation, although the solution did not converge. The use of polyhedron mesh to reduce the number of elements and increase the number of computational nodes to achieve faster convergence and improve mesh quality features was then introduced to improve numerical solution behaviour, however, this strategy also failed to offer the required convergence.

Finally, the hexagonal mesh was used using ICEM CFD 19.2 to provide the highest quality meshing in terms of aspect ratio, skewness, and orthogonality as shown in Figure 6(a) and Figure 6(b)

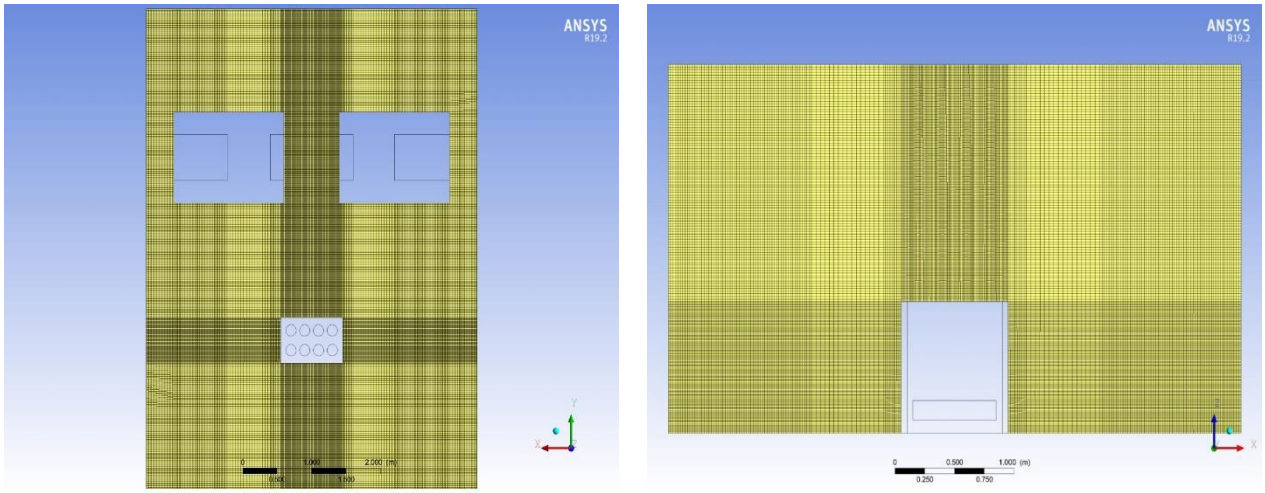

(a) (b)

Fig. 6. (a) Meshing top view cross-section on X-Y plane (b) Meshing top view cross-section on Z-X plane

On the current study, it was detected that the aspect ratio had a discernible effect on solution convergence as its value greater than (20) had a significant effect on convergence; hence, numerous attempts have been made to modify the aspect ratio to a value not exceeding 6. Good convergence requirements are 10^{-10} for the energy conservation equation, 10^{-5} for continuity, and 10^{-6} for k, ε equations as shown in Figure 7.

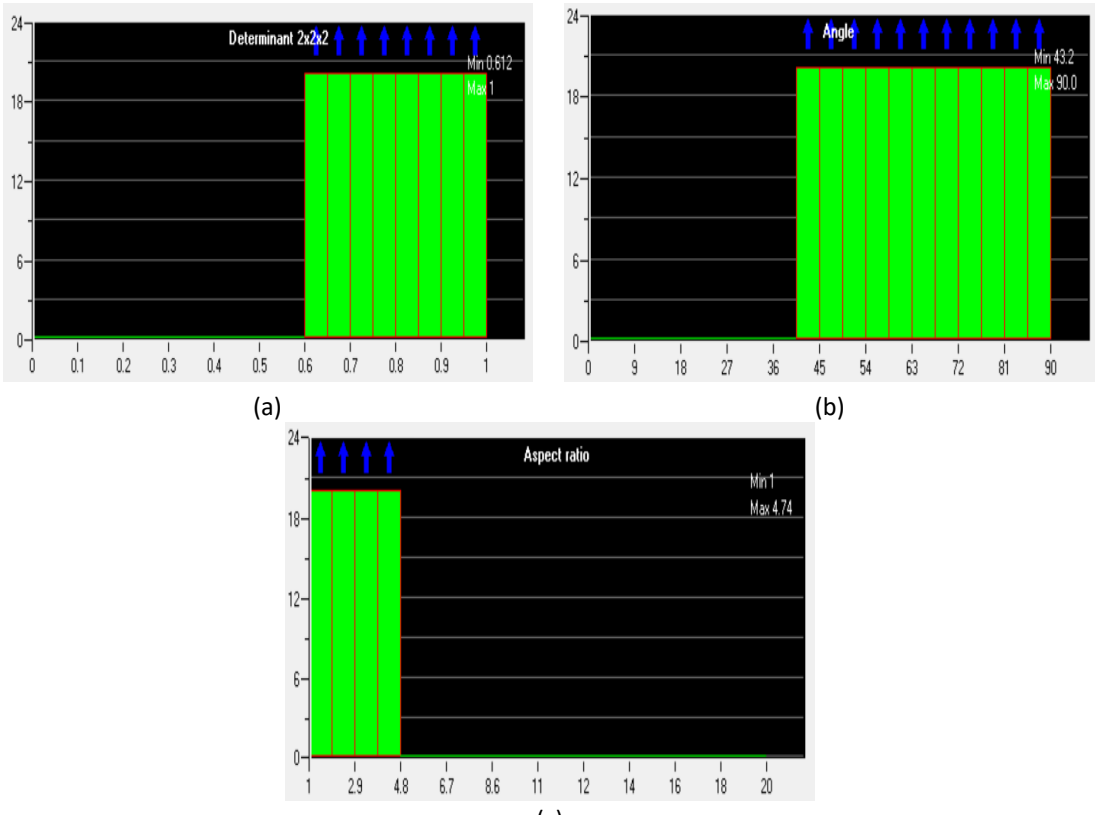

(a) (b)

(c)

Fig. 7. (a) Meshing quality report (b) Meshing angle criterion report (c) Meshing aspect ratio criterion report

2.2.6 Model validation

Validation is required to assess the simulation's accuracy. The simulation of the airflow characteristics and temperature distribution for a typical thermal situation was performed with the same boundary condition as in Lin *et al.,* [5] and the results were compared to those of Lin *et al.,* [5]. To check the agreement of validation with experimental work, a specified zone area around and above the process tool is well marked, as in Figure 8. Several (500) well-specified points along a horizontal line at a height of 0.4 m above the process tool are used to draw a curve representing the variation of the temperature distribution index Θ throughout the specified.

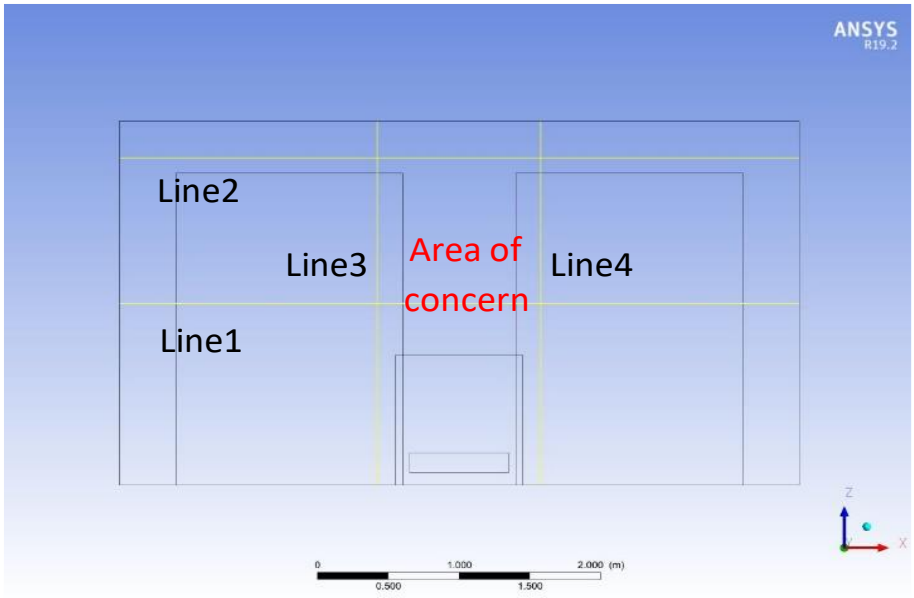

(a)

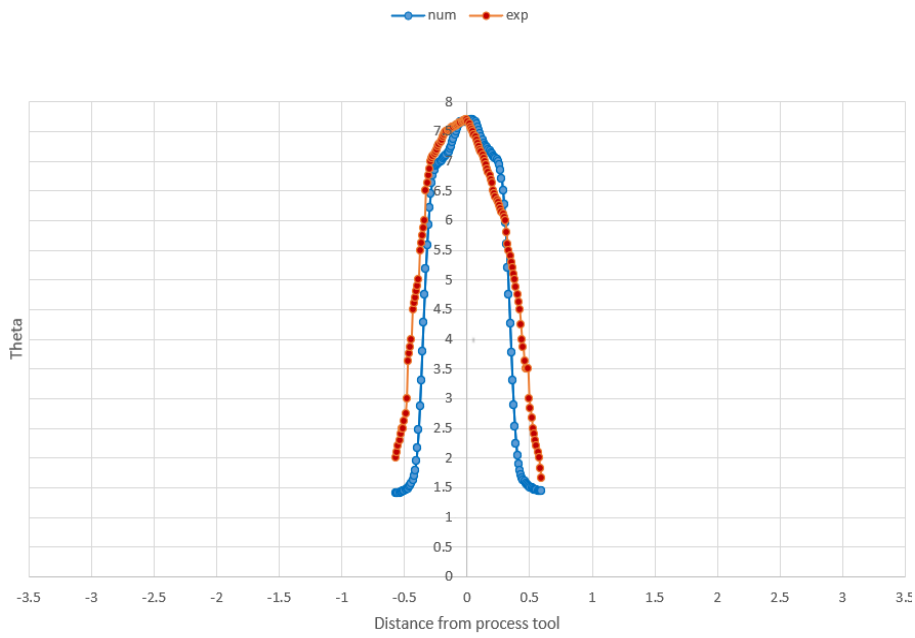

(b)

Fig. 8. (a) Area bounded by lines (1-4) over and around process tool (b) Result of experiment and numerical solution for wall return air system

To quantify the performance of the model, a statistical method known as the index of agreement Eq. (1) was developed. It was proposed by Willmott (1981) as a standardized measure of the degree of model prediction error, and it fluctuates between 0 and 1. The agreement index is the ratio between the mean square error and the potential error. A score of 1 for agreement implies a perfect match, whereas a value of 0 shows no agreement at all.

$$IA = 1 - \frac{\sum_{i=1}^{P}(x_i - y_i)^2}{\sum_{i}^{P}(|y_i - x_m| + |x_i - x_m|)^2} \quad (1)$$

where x_i represents the measurements, y_i represents the numerical values, and p is the total number of experimental test points. When the result value is (1) for IA, it shows that the simulation results agree well with the measurements as shown in Figure 9.

IA's value is 0.932, which is close to one. Figure 9 demonstrates that the simulation findings are compatible with the experimental results, indicating that the numerical model is reliable for calculating the various air characteristics of wall return ventilation in different scenarios.

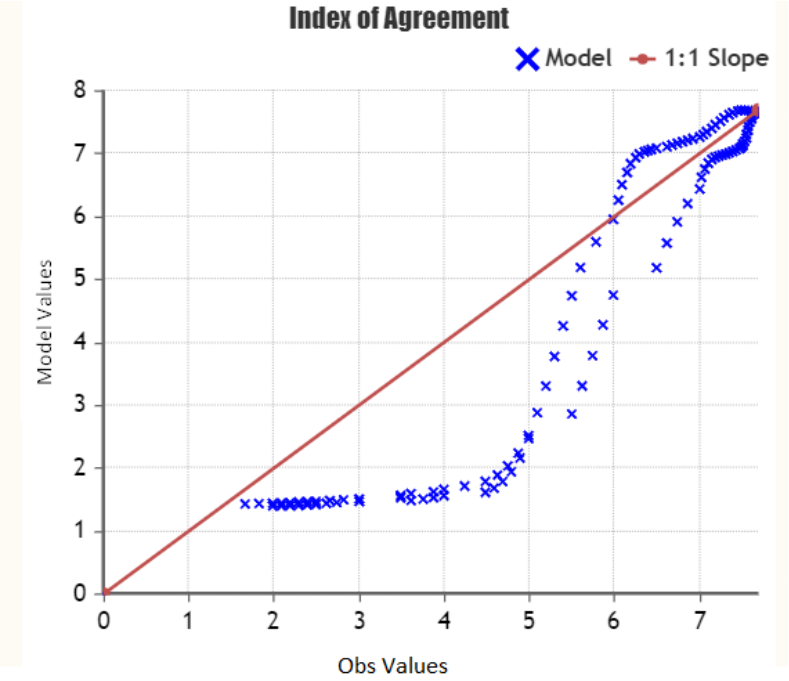

Fig. 9. Index of agreement of experiment and numerical solution for wall return

2.2.7 Mesh sensitivity analysis

The impact of mesh size on numerical solution convergence and agreement with experimental results was investigated using three mesh sizes as shown in Table 2. The three sizes of meshing are as follows:

Table 2
Mesh sizes used for sensitivity analysis

	Coarse	Medium	Fine
Number of Elements	12,358,145	17,537,904	20,257,968
Number of Nodes	12,595,152	17,830,442	20,578,872

The mesh sensitivity analysis is made using the average local air temperature index value Θ in the selected area above the manufacturing process tool Figure 7(a).

From the mesh sensitivity analysis as shown in Figure 10 and comparison of experimental work results with numerical solution result for the wall return air system, it was noticed that the difference in solution results between coarse mesh and medium mesh is about 0.01 % and the difference between medium mesh and a fine mesh is about 0.02 %. So, medium mesh size is used in the validation study and throws out this research. Furthermore, the numerical simulation of medium mesh size gives a good agreement with the experimental value of average Θ for the wall return air system, which deviates about 11%. This value of deviation is good as compared to previous similar validation analyses for expecting air flow characteristics and temperature distribution for different ventilation systems.

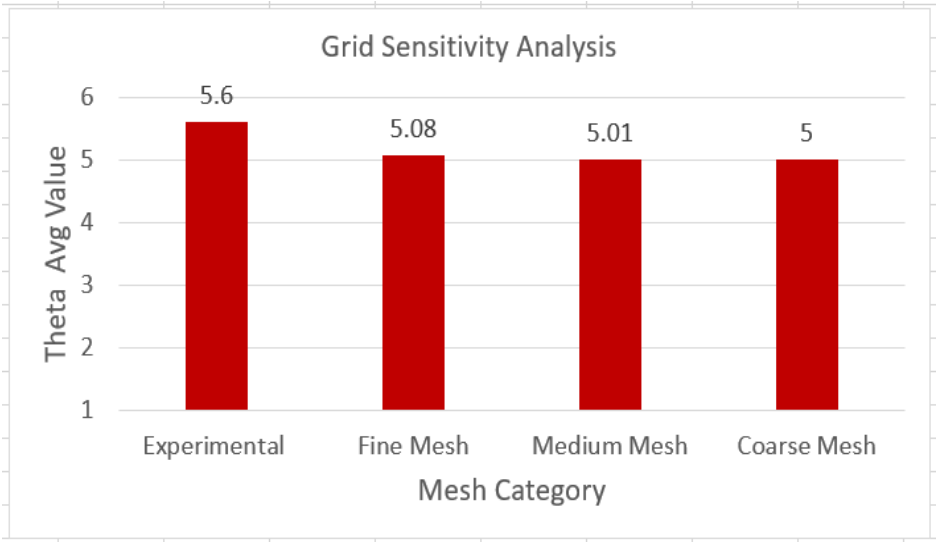

Fig. 10. Comparison between the experimental average Θ and the average Θ of numerical solution of different mesh sizes for a wall-return ventilation system

3. Results and Discussion

A comprehensive examination of the numerical simulation results for a class 1000 clean room utilized in the electronic manufacturing process. The wall returns, ARR-1, ARR-2, and ARR-3 cleanroom models have been examined. The findings of the local air temperature index Θ are depicted in Figure 11 and Figure 12 for two distinct cross sections labelled A-A and B-B. In addition, Figure 12 and Table 3 present a comparison between the values of the local air temperature index Θ across the cleanroom and the aforementioned process tool. Lastly, another comparison of wall returns and FDCU-selected cases, as shown in Table 4 and Table 5, has been conducted.

Figure 11 and Figure 12 depict the local air temperature index for two cross sections A-A and B-B on the y-z and x-z axes, respectively. Higher values were observed above the process tool, on a specified zone of interest at X/L = 0.4-0.6 and Y/W = 0.45-0.55, as shown in Figure 8(a), and this value varies with distance away from the process tool based on the position of the process tool relative to the cooling downward supply air from the FFU.

Due to the combination of the high velocity of tool exhaust in the designated region and the action of forced convection on the process tool, this region is characterized by a heightened temperature gradient. The collision between the downward airflow from the central FFU and the upward high-velocity exhaust from the tool caused the hot plume to spread along the ceiling, as

depicted in Figure 11 and Figure 12, with less high-temperature contours spreading through the room and the ceiling area in case ARR-3, as depicted in Figure 11(d) and Figure 12(d).

The Θ values, in the FDCU-return and wall-return air systems were completely different, in addition, the shape of the temperature contours width and spreading is a good measure of the effectiveness of the proposed ventilation system. Lastly, the Θ value is a good indicator of the relationship between T_{local} at any position within the cleanroom and T_{return}; hence, it is a good indicator that the hot air drained from the process tool has been thoroughly mixed with the cold air supply in the cleanroom before being exhausted.

The local air temperature index Θ contours in Figure 11(a) and Figure 12(a) indicate that the wall return ventilation system is responsible for the dispersion of heat generated by the manufacturing process tool within the cleanroom. These contours cover broad floor-to-ceiling regions at nearly all room heights. The diameter of the heat plume is considerably greater than in situations where the FDCU ventilation system is utilized.

On ARR-1 to ARR-3, an FDCU return air system is utilised, as depicted in Figure 11(b)-(d), Figure 12(b)-(d), and it is evident from these figures that the arrangement of FDCU units in relation to FFU has a significant impact on the shape of the heat plume and the distribution of heat contours within the cleanroom.

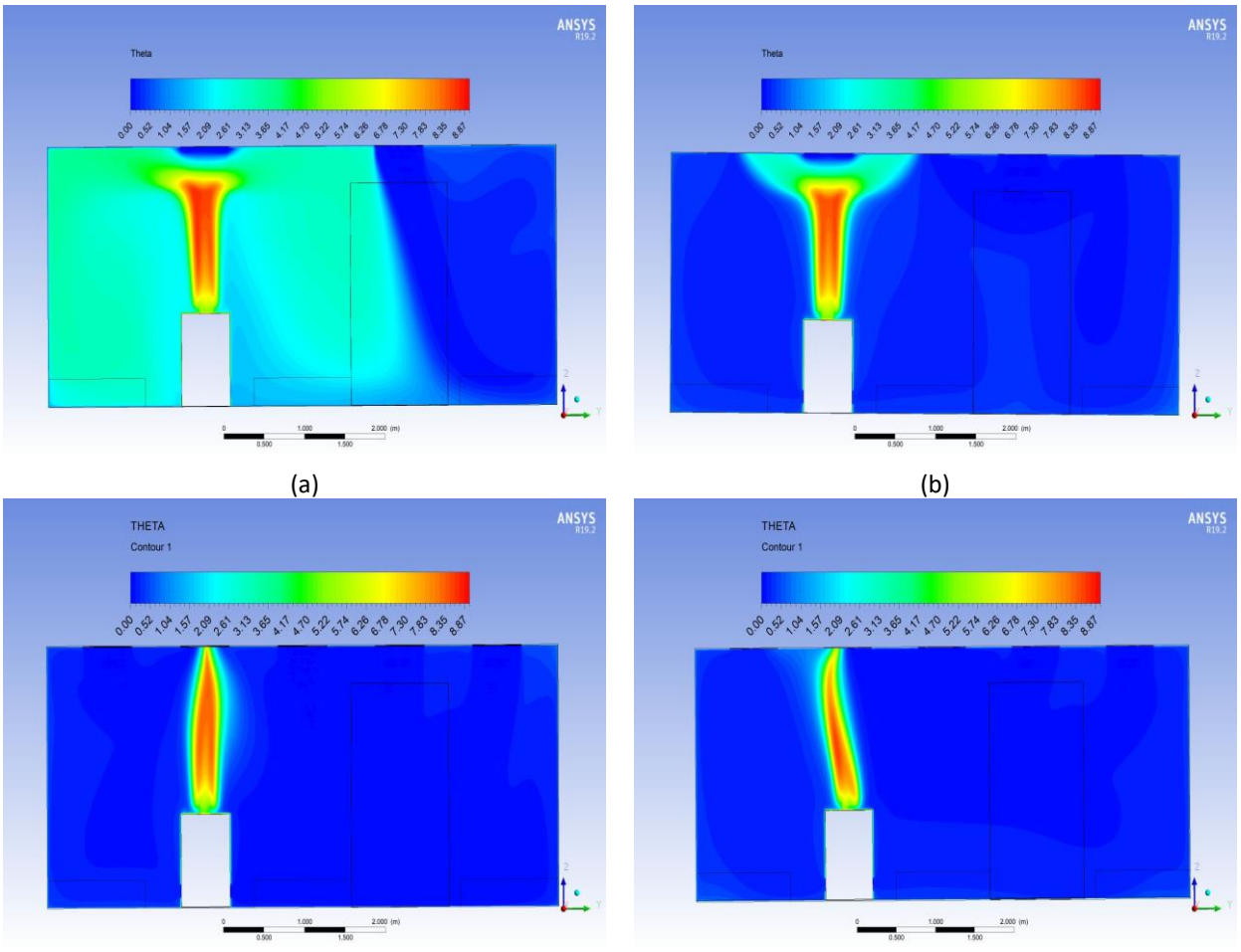

Fig. 11. Local air temperature index Θ at section A-A for (a) Wall return, (b) ARR-1, (c) ARR-2, (d) ARR-3

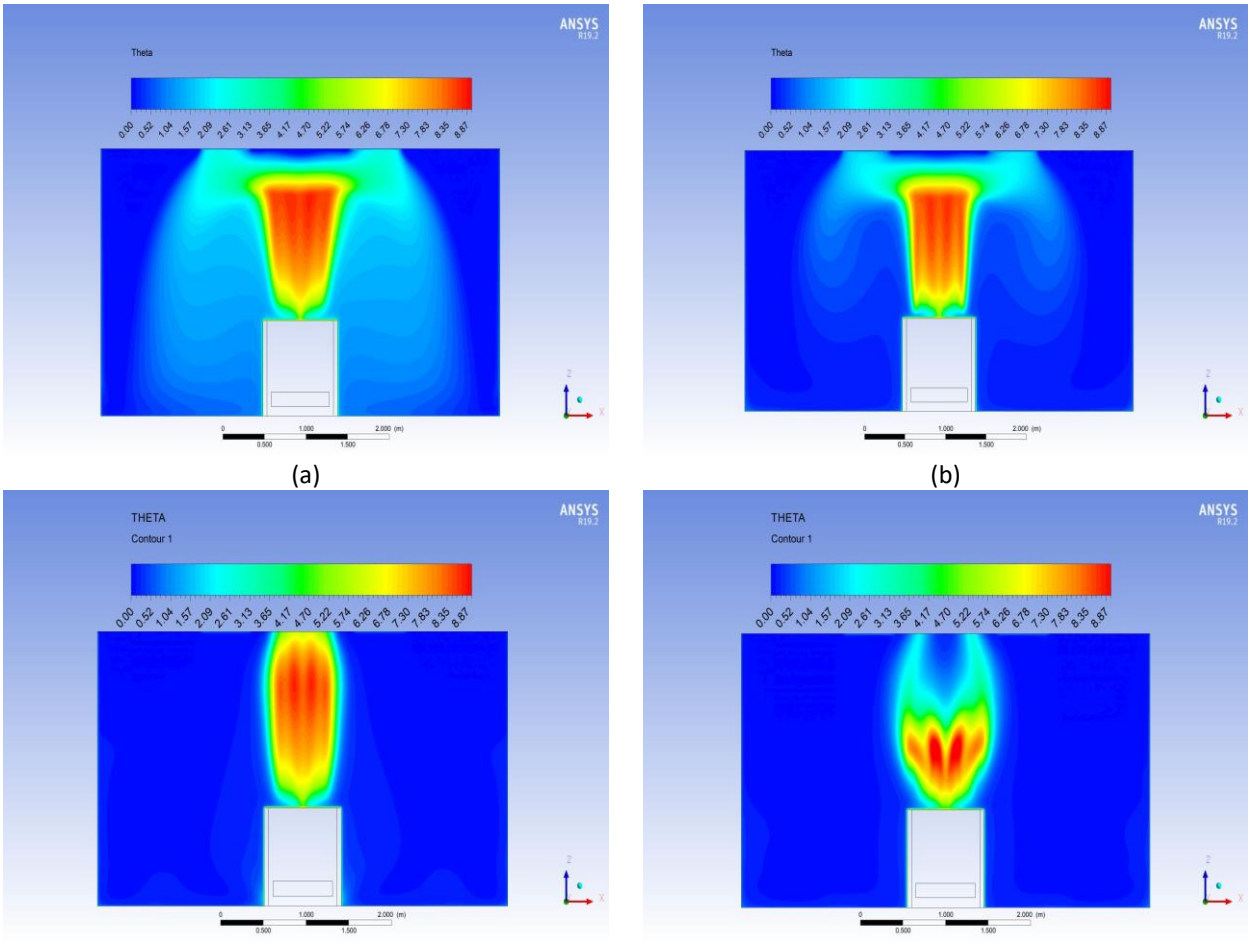

Fig. 12. Local air temperature index Θ at section B-B for (a) Wall return (b) ARR-1 (c) ARR-2 (d) ARR-3

Figure 13 and Table 3 summarize all the characteristics utilized to compare conventional wall return to the various FDCU ventilation system configurations. The location of the FDCU has a considerable impact on the value of the local air temperature index above the process tool and also regulates the distribution of heat throughout the cleanroom. In addition, the FDCU ventilation system appears to have a big impact on the contours of the heat plume above the process tool.

To determine the efficiency of the FDCU return air system in removing heat from the clean room and the zone of interest above the manufacturing process tool, a comparison is made between wall return (case 1) and the suggested FDCU arrangement (ARR-2 and ARR-3) using the wall return as a baseline. Comparing ARR-3 to ARR-2 and the wall return air system, Table 4 reveals that ARR-3 is the most effective. Furthermore, a comparison with ARR-1, which was experimentally demonstrated reveals that ARR-2 and ARR-3 are effective in removing more heat from the area of concern above the process tool and from the clean room as a whole.

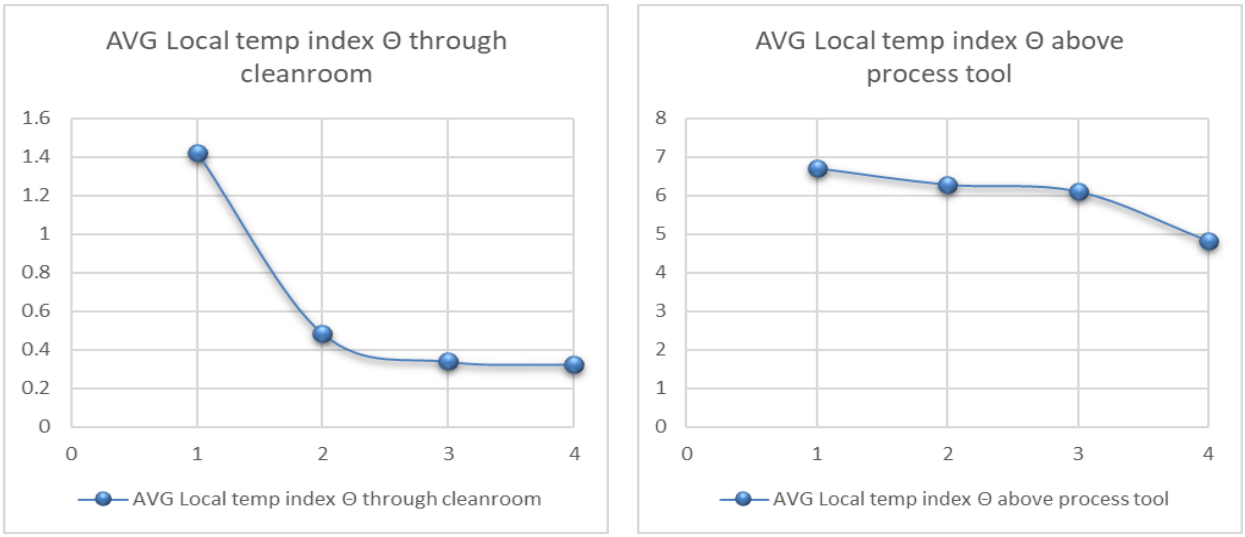

(a) (b)

Fig. 13. (a) Local temp. index through the cleanroom (b) Local temp. an index above the process tool

Table 3
Summary of local air temperature index Θ and turbulence intensity through all cleanroom and through a specified zone of interest above process tool

	AVG Local temp index Θ through the cleanroom	AVG Local temp index Θ above process tool
Wall returns	1.4193	6.71438
ARR-1	0.48333	6.28724
ARR-2	0.338719	6.10731
ARR-3	0.324086	4.81717

Table 4
Comparison between ARR-2 and ARR-3 and wall return for local air temperature index Θ through all cleanrooms and a specified zone of interest above process tool

	AVG Local temp index Θ through the cleanroom	AVG Local temp index Θ above process tool
ARR-2 vs wall-return	-76%	-9%
ARR-3 vs wall-return	-77%	-28%

Table 5
Comparison between ARR-2 and ARR-3 and ARR-1 for local air temperature index Θ through all cleanrooms and a specified zone of interest above process tool

	AVG Local temp index Θ through the cleanroom	AVG Local temp index Θ above process tool
ARR-2 vs ARR-1	-30%	-3%
ARR-2 vs ARR-1	-33%	-23%

4. Conclusions

This study explores quantitatively the effectiveness of a new FDCU return air system in removing heat and preventing its spread within an industrial cleanroom including process instruments that generate particles and dissipate high-temperature heat. This system is comprised of ceiling-mounted supply and return fan coils. In addition, the analysis depicts the impact of relocating the FDCU on the temperature distribution within the cleanroom. The previously described industrial cleanroom has a width of 4.8 meters, a length of 6.3 meters, and a height of 2.8 meters, and it contains a production process tool that expels heat and contaminants from the workstation. The setting of the model was

identical to that of the actual experiment [5]. Following are the key findings of the study based on the acquired data

i. Locating FFU just above the process tool is not a preferred location as the interaction of FFU supply downward air and process tool exhaust upward air increases turbulence in this area and has a major effect on spreading heat and contaminants throughout the cleanroom [5].
ii. Placing at least one FDCU above the manufacturing process tool in ARR-2 and ARR-3 dramatically improves the dispersion of heat and pollutants within the cleanroom, as shown in Figure 11, Figure 12, Table 4 and Table 5.
iii. Compared to the standard wall return ventilation system, the FDCU ARR-3 can exhaust 76% of the heat from the region above the process tool and 28% of the heat from the cleanroom.
iv. Compared to FDCU ARR-1, FDCU ARR-3 can exhaust 33% of the heat from the area above the process tool and 23% from within the cleanroom, as demonstrated experimentally [5].

Acknowledgment
This research was not funded by any grant.

References

[1] Shih, Hui-Ya, Shih-Hsuan Huang, Shou-Nan Li, Sheng-Chieh Chen, and Chuen-Jinn Tsai. "Simulation and testing of pollutant dispersion during preventive maintenance in a cleanroom." *Building and environment* 44, no. 12 (2009): 2319-2326. https://doi.org/10.1016/j.buildenv.2009.03.018
[2] Shih, Yang-Cheng, An-Shik Yang, and Chang-Wei Lu. "Using air curtain to control pollutant spreading for emergency management in a cleanroom." *Building and Environment* 46, no. 5 (2011): 1104-1114. https://doi.org/10.1016/j.buildenv.2010.11.011
[3] Vutla, Srinivasa Rao, Srinivasa Prakash Regalla, and Kannan Ramaswamy. "Life cycle assessment of cleanroom for micro-electro-mechanical systems fabrication with insights on sustainability." *Journal of Cleaner Production* 282 (2021): 124520. https://doi.org/10.1016/j.jclepro.2020.124520
[4] Lin, Ti, Yun-Chun Tung, Shih-Cheng Hu, and Chen-Yen Lin. "Effects of the Removal of 0.1 µm Particles in Industrial Cleanrooms with a Fan Dry Coil Unit (FDCU) Return System." *Aerosol and air quality research* 10, no. 6 (2010): 571-580. https://doi.org/10.4209/aaqr.2010.03.0014
[5] Lin, Ti, Yun-Chun Tung, Shih-Cheng Hu, and Yen-Jhih Chen. "Experimental study on airflow characteristics and temperature distribution in non-unidirectional cleanrooms for electronic industry." *Building and Environment* 46, no. 6 (2011): 1235-1242. https://doi.org/10.1016/j.buildenv.2010.10.028
[6] Tung, Yun-Chun, Shih-Cheng Hu, Tengfang Xu, and Ren-Huei Wang. "Influence of ventilation arrangements on particle removal in industrial cleanrooms with various tool coverage." In *Building Simulation*, vol. 3, pp. 3-13. Tsinghua Press, 2010. https://doi.org/10.1007/s12273-010-0301-z
[7] Lin, Ti, Shih-Cheng Hu, Andy Chang, and Cheng-Yan Lin. "An Innovative Ventilation System for Cleanrooms with High Cooling Loads." *ASHRAE Transactions* 116, no. 1 (2010).
[8] Xu, Tengfang, Chao-Ho Lan, and Ming-Shan Jeng. "Performance of large fan-filter units for cleanroom applications." *Building and Environment* 42, no. 6 (2007): 2299-2304. https://doi.org/10.1016/j.buildenv.2006.05.007
[9] Chen, Juhn-Jie, Chao-Ho Lan, Ming-Shan Jeng, and Tengfang Xu. "The development of fan filter unit with flow rate feedback control in a cleanroom." *Building and Environment* 42, no. 10 (2007): 3556-3561. https://doi.org/10.1016/j.buildenv.2006.10.026
[10] Shao, Xiaoliang, Shukui Liang, Jiaan Zhao, Huan Wang, Huifang Fan, Hui Zhang, Guanpeng Cao, and Xianting Li. "Experimental investigation of particle dispersion in cleanrooms of electronic industry under different area ratios and speeds of fan filter units." *Journal of Building Engineering* 43 (2021): 102590. https://doi.org/10.1016/j.jobe.2021.102590
[11] Zhao, Jiaan, Chenjiyu Liang, Huan Wang, Xianting Li, and Wei Xu. "Control strategy of fan filter units based on personnel position in semiconductor fabs." *Building and Environment* 223 (2022): 109420. https://doi.org/10.1016/j.buildenv.2022.109420

[12] Shao, Xiaoliang, Yunfeng Hao, Shukui Liang, Huan Wang, Yu Liu, and Xianting Li. "Experimental characterization of particle distribution during the process of reducing the air supply volume in an electronic industry cleanroom." *Journal of Building Engineering* 45 (2022): 103594. https://doi.org/10.1016/j.jobe.2021.103594
[13] Murakami, Shuzo, Shinsuke Kato, and Yoshimi Suyama. "Numerical and experimental study on turbulent diffusion fields in conventional flow type clean rooms." *Ashrae Transactions* 94, no. 2 (1988): 469-493.
[14] Murakami, S., S. Kato, and Y. Suyama. "Numerical study on diffusion field as affected by arrangement of supply and exhaust openings in conventional flow type clean room." *ASHRAE Transactions* 95, no. 2 (1989): 113-127.
[15] Murakami, S., S. Kato, S. Nagano, and Y. J. A. T. Tanaka. "Diffusion characteristics of airborne particles with gravitational settling in a convection-dominant indoor flow field." *Ashrae Transactions* 98, no. 1 (1992): 82-97.
[16] Kato, S., S. Murakami, and S. Nagano. "Numerical study on diffusion in a room with a locally balanced supply exhaust airflow rate system." *ASHRAE transactions* 98, no. 1 (1992): 218-238.
[17] Zhao, Fu-Yun, Jin Cheng, Bao Liu, Zhi-Rong Huang, and Xianting Li. "Indoor airflow and pollutant spread inside the cleanroom with micro-porous supplying panel and different ventilation schemes: Analytical, numerical and experimental investigations." *Journal of Building Engineering* 31 (2020): 101405. https://doi.org/10.1016/j.jobe.2020.101405
[18] Qin, Chao, and Wei-Zhen Lu. "Effects of ceiling exhaust location on thermal comfort and age of air in room under impinging jet supply scheme." *Journal of Building Engineering* 35 (2021): 101966. https://doi.org/10.1016/j.jobe.2020.101966
[19] Ljungqvist, Bengt. "Some observations of the interaction between air movements and the dispersion of pollution." (1979).
[20] Milberg, Joachim, Johannes Fischbacher, and Andreas Engel. "Fluidic integration of equipment in cleanrooms." *Solid State Technology* 34, no. 8 (1991): 43-47.
[21] Zhao, Jiaan, Xiaoliang Shao, Xianting Li, Chao Liang, Huan Wang, and Wei Xu. "Theoretical expression for clean air volume in cleanrooms with non-uniform environments." *Building and Environment* 204 (2021): 108168. https://doi.org/10.1016/j.buildenv.2021.108168
[22] Kuehn, Thomas. "Computer simulation of airflow and particle transport in cleanrooms." *The Journal of Environmental Sciences* 31, no. 5 (1988): 21-27. https://doi.org/10.17764/jiet.1.31.5.464773718u8051x2
[23] Kuehn, T. H., V. A. Marple, H. Han, D. Liu, I. Shanmugavelu, and S. W. Youssef. "Comparison of measured and predicted airflow patterns in a clean room." In *34th annual technical meeting of the Institute of Environmental Sciences*, pp. 98-107. 1988.
[24] Fujii, S., K. Yuasa, Y. Arai, T. Watanabe, and Y. Suwa. "Characteristics of airflow turbulence behind HEPA filter." In *Contamination control, symposium on minienvironments, symposium on biocontamination control. 1994 proceedings, Volume 1*. 1994.
[25] Hu, S. C., Y. Y. Wu, and C. J. Liu. "Measurements of air flow characteristics in a full-scale clean room." *Building and Environment* 31, no. 2 (1996): 119-128. https://doi.org/10.1016/0360-1323(95)00039-9
[26] Whyte, W., M. Hejab, W. M. Whyte, and G. Green. "Experimental and CFD airflow studies of a cleanroom with special respect to air supply inlets." *International Journal of Ventilation* 9, no. 3 (2010): 197-209. https://doi.org/10.1080/14733315.2010.11683880
[27] Lin, Tee, Shih-Cheng Hu, and Tengfang Xu. "Developing an innovative fan dry coil unit (FDCU) return system to improve energy efficiency of environmental control for mission critical cleanrooms." *Energy and Buildings* 90 (2015): 94-105. https://doi.org/10.1016/j.enbuild.2014.12.003
[28] El-Haroun, Ahmed Fahmy, Sayed Ahmed Kaseb, Mahmoud Ahmed Fouad, and Hatem Omar Kayed. "Numerical Investigation of Covid-19 Infection Spread Expelled from Cough in an Isolation Ward Under Different Air Distribution Strategies." *Journal of Advanced Research in Fluid Mechanics and Thermal Sciences* 95, no. 1 (2022): 17-35. https://doi.org/10.37934/arfmts.95.1.1735
[29] Winata, I. Made Putra Arya, Putu Emilia Dewi, Putu Brahmanda Sudarsana, and Made Sucipta. "Air-Flow Simulation in Child Respirator for Covid-19 Personal Protection Equipment Using Bamboo-Based Activated Carbon Filter." *Journal of Advanced Research in Fluid Mechanics and Thermal Sciences* 91, no. 1 (2022): 83-91. https://doi.org/10.37934/arfmts.91.1.8391
[30] Sannad, Mohamed, Youcef Mehdi, Afaf Zaza, Youness El Hammami, Youssef Idihya, and Othmane Benkortbi. "A Numerical Simulation Under Milk Fouling in A Plate Heat Exchanger in The Presence of a Porous Medium." *Journal of Advanced Research in Fluid Mechanics and Thermal Sciences* 91, no. 1 (2022): 1-17. https://doi.org/10.37934/arfmts.91.1.117
[31] Qing, Nelvin Kaw Chee, Nor Afzanizam Samiran, and Razlin Abd Rashid. "CFD Simulation analysis of Sub-Component in Municipal Solid Waste Gasification using Plasma Downdraft Technique." *CFD Letters* 14, no. 8 (2022): 63-70. https://doi.org/10.37934/cfdl.14.8.6370